Molecular Microbiology (2007) **64**(3), 676–690 doi:10.1111/j.1365-2958.2007.05686.x

The rotational dynamics of kinetoplast DNA replication

Yanan Liu and Paul T. Englund*
Department of Biological Chemistry, Johns Hopkins Medical School, Baltimore, MD, USA.

Summary

Kinetoplast DNA (kDNA), from trypanosomatid mitochondria, is a network containing several thousand catenated minicircles that is condensed into a disk-shaped structure *in vivo*. kDNA synthesis involves release of individual minicircles from the network, replication of the free minicircles and reattachment of progeny at two sites on the network periphery ~180° apart. In *Crithidia fasciculata*, rotation of the kDNA disk relative to the antipodal attachment sites results in distribution of progeny minicircles in a ring around the network periphery. In contrast, *Trypanosoma brucei* progeny minicircles accumulate on opposite ends of the kDNA disk, a pattern that did not suggest kinetoplast motion. Thus, there seemed to be two distinct replication mechanisms. Based on fluorescence microscopy of the kDNA network undergoing replication, we now report that the *T. brucei* kinetoplast does move relative to the antipodal sites. Whereas the *C. fasciculata* kinetoplast rotates, that from *T. brucei* oscillates. Kinetoplast motion of either type must facilitate orderly replication of this incredibly complex structure.

Introduction

Trypanosomes are protozoan parasites that cause important tropical diseases. One of their fascinating features is their mitochondrial DNA, known as kinetoplast DNA (kDNA), which is a massive network of topologically interlocked DNA circles. The *Trypanosoma brucei* kDNA network consists of several thousand 1 kb minicircles that are heterogeneous in sequence and a few dozen 23 kb maxicircles. Maxicircles, like mitochondrial DNAs of higher organisms, encode rRNA and proteins such as some subunits of respiratory complexes. Minicircles encode guide RNAs involved in editing of maxicircle transcripts. See (Stuart *et al*., 2005) for a review on editing. The kDNA *in vivo* is condensed into a disk-shaped structure positioned in the mitochondrial matrix near the flagellar basal body. There is a *trans*-membrane filament system linking the kDNA disk to the basal body that facilitates segregation of daughter networks (Robinson and Gull, 1991; Ogbadoyi *et al*., 2003). Network replication has been well studied in *Crithidia fasciculata* and *T. brucei* and the current working model for this process, focusing on minicircles, is presented in the following paragraph. A key feature of kDNA replication, which contributes to its complexity, is that it must provide for proper segregation of minicircles; if this was not the case, minicircle species would be lost, maxicircle editing could not function without essential guide RNAs, and the cells would lose viability. See (Shlomai, 2004; Liu *et al*., 2005a) for reviews on kDNA.

Prior to replication, all minicircles in the network are covalently closed. When replication begins, covalently closed minicircles are individually released from the network into the kinetoflagellar zone [KFZ, a region between the kDNA disk and the mitochondrial membrane near the flagellar basal body (Drew and Englund, 2001)]. Proteins localized in the KFZ promote initiation of replication of the free minicircles; these proteins include the universal minicircle sequence-binding protein [UMSBP, that binds the replication origin (Abu-Elneel *et al*., 2001)], DNA primase (Li and Englund, 1997) and two DNA polymerases (Klingbeil *et al*., 2002a). After replication of the free minicircles as θ-structures, their progeny migrate from the KFZ to the antipodal sites, two protein assemblies that are of key importance to the work reported here. The antipodal sites flank the kDNA disk and are positioned ~180° apart. They contain enzymes that catalyse some of the later reactions in minicircle replication. These include removal of RNA primers by a structure-specific endonuclease-I (SSE1) (Engel and Ray, 1998; 1999; Liu *et al*., 2005b) and repair of some (but not all) of the minicircle gaps by a DNA polymerase β (Ferguson *et al*., 1992; Torri and Englund, 1995) and a DNA ligase (Downey *et al*., 2005). Finally, a topoisomerase II, also in the antipodal sites, attaches the progeny minicircles (each containing at least one gap) to two peripheral positions on the kDNA network, adjacent to the antipodal sites (Melendy *et al*., 1988; Wang and Englund, 2001). Another protein localized in or near the antipodal sites, p38, appears to function in initiation of minicircle replication; it may migrate to the KFZ for this purpose (Liu *et al*., 2006). As replication proceeds, there is enlargement of the network's peripheral zones containing gapped minicircles that have already replicated; there is a corresponding shrinkage of the central zone containing covalently closed

Accepted 1 March, 2007. *For correspondence. E-mail penglund@jhmi.edu; Tel. (+1) 410 955 3790; Fax (+1) 410 955 7810.

minicircles that have not yet replicated. Thus, the network grows until every minicircle has replicated and their copy number has doubled. When replication is complete, the remaining gaps are repaired, the double-size network splits in two, and the progeny networks segregate into the daughter cells (Hoeijmakers and Weijers, 1980; Pérez-Morga and Englund, 1993a; Ferguson *et al*., 1994; Robinson and Gull, 1994; Guilbride and Englund, 1998).

Trypanosoma brucei and *C. fasciculata* differ markedly in the pattern of attachment of progeny minicircles to the network. In *T. brucei*, the gapped progeny minicircles accumulate at two peripheral regions ~180° apart (Hoeijmakers and Weijers, 1980; Ferguson *et al*., 1994; Robinson and Gull, 1994; Guilbride and Englund, 1998). In *C. fasciculata*, on the other hand, the gapped progeny minicircles distribute in a ring around the network periphery (Simpson *et al*., 1974; Simpson and Simpson, 1976; Englund, 1978; Ferguson *et al*., 1992; Pérez-Morga and Englund, 1993b). It is straightforward to explain how gapped minicircles localize to the network poles in *T. brucei*, because they accumulate near the two antipodal sites where they were attached. A more complex explanation was needed for the ring pattern in *C. fasciculata*. EM-autoradiography of networks pulse-labelled metabolically for various times with [^{3}H]thymidine revealed that newly replicated minicircles, as in *T. brucei,* are attached to the network periphery at positions ~180° apart. Then relative motion of the kDNA disk and the two antipodal minicircle attachment sites distributed the newly replicated minicircles in a peripheral ring. We proposed that the kDNA disk actually rotated between fixed antipodal sites (Pérez-Morga and Englund, 1993b). Also see (Simpson *et al*., 1974; Simpson and Simpson, 1976).

Here we describe the structural organization of replicating kDNA networks using fluorescence methods. We found that the *T. brucei* kinetoplast is not stationary as previously thought, but that it moves relative to the fixed antipodal sites. This motion differs from that in *C. fasciculata*; instead of rotating, the *T. brucei* kinetoplast oscillates, thereby distributing the newly replicated minicircles along a limited region of the periphery at each end of the network. Unexpectedly, we also found that RNAi silencing of several *T. brucei* kDNA replication proteins alters the pattern of kinetoplast motion.

Results

A fluorescence method for studying the dynamics of C. fasciculata *kDNA network replication*

Our experimental approach is to label cultured cells for various times with bromodeoxyuridine (BrdU) (Woodward and Gull, 1990; Robinson and Gull, 1994). This thymidine analogue is incorporated into replicating free minicircles whose progeny then attach to the kDNA network. After purification of the networks, we use terminal deoxynucleotidyl transferase (TdT) and a fluorescent deoxynucleoside triphosphate to tag 3′-OH groups at minicircle gaps (Guilbride and Englund, 1998; Johnson and Englund, 1998; Drew and Englund, 2001). Acid treatment of the isolated kDNA then exposes the BrdU epitopes for immunodetection with fluorescently tagged anti-BrdU antibody. Fluorescence microscopy reveals the network regions already replicated during the current cell cycle (green TdT label) as well as the region that was replicated during the pulse (red BrdU label). Usually the area of TdT labelling exceeds that of BrdU labelling because the network replication was already underway when the BrdU pulse labelling was initiated.

We first tested this protocol on *C. fasciculata* kDNA as there was already considerable knowledge of its replication dynamics. We pulsed cells with BrdU for 3 min, and then labelled isolated networks with TdT (Fig. 1A, networks a, b and c). In these networks the green TdT label either forms a thin ring (network a, at an early stage of replication), a thicker ring (network b, at a later stage), or the label virtually fills the network (network c, in the final stage). However, in all three the red BrdU fluorescence is limited to two peripheral zones ~180° apart, as expected if the BrdU-labelled minicircles are attached next to the antipodal sites. When the BrdU labelling is increased to 30 min (Fig. 1A, networks d and e), the red fluorescense covers the entire network periphery, consistent with movement of the kinetoplast relative to the antipodal sites (Pérez-Morga and Englund, 1993b). When labelling is 1 h or 2 h (Fig. 1A, networks f, g and h), there is a corresponding increase in thickness of the ring of BrdU-labelled minicircles, consistent with multiple rotations of the kinetoplast during the labelling period. These studies demonstrate that this fluorescence method provides excellent visualization of the replication dynamics of *C. fasciculata* kDNA, and the results confirm previous studies involving EM-autoradiography of [^{3}H]thymidine-labelled networks (Pérez-Morga and Englund, 1993b).

We next used fluorescence methods to obtain new information about *C. fasciculata* kDNA replication. Instead of labelling isolated networks, we fixed and permeabilized cells and then labelled them *in situ* with TdT and DAPI. Under these conditions, TdT labels the antipodal sites very strongly because they are enriched in multiply gapped free minicircles. In contrast, TdT labels more weakly the regions of the kDNA disk containing gapped minicircles because most of the gaps in free minicircles had been repaired just prior to network attachment (Johnson and Englund, 1998). As shown in Fig. 1B, kinetoplasts *in situ* had several configurations. Some like that in panel a were TdT negative. Others, like that in panel b had strong TdT labelling in the antipodal sites but little in

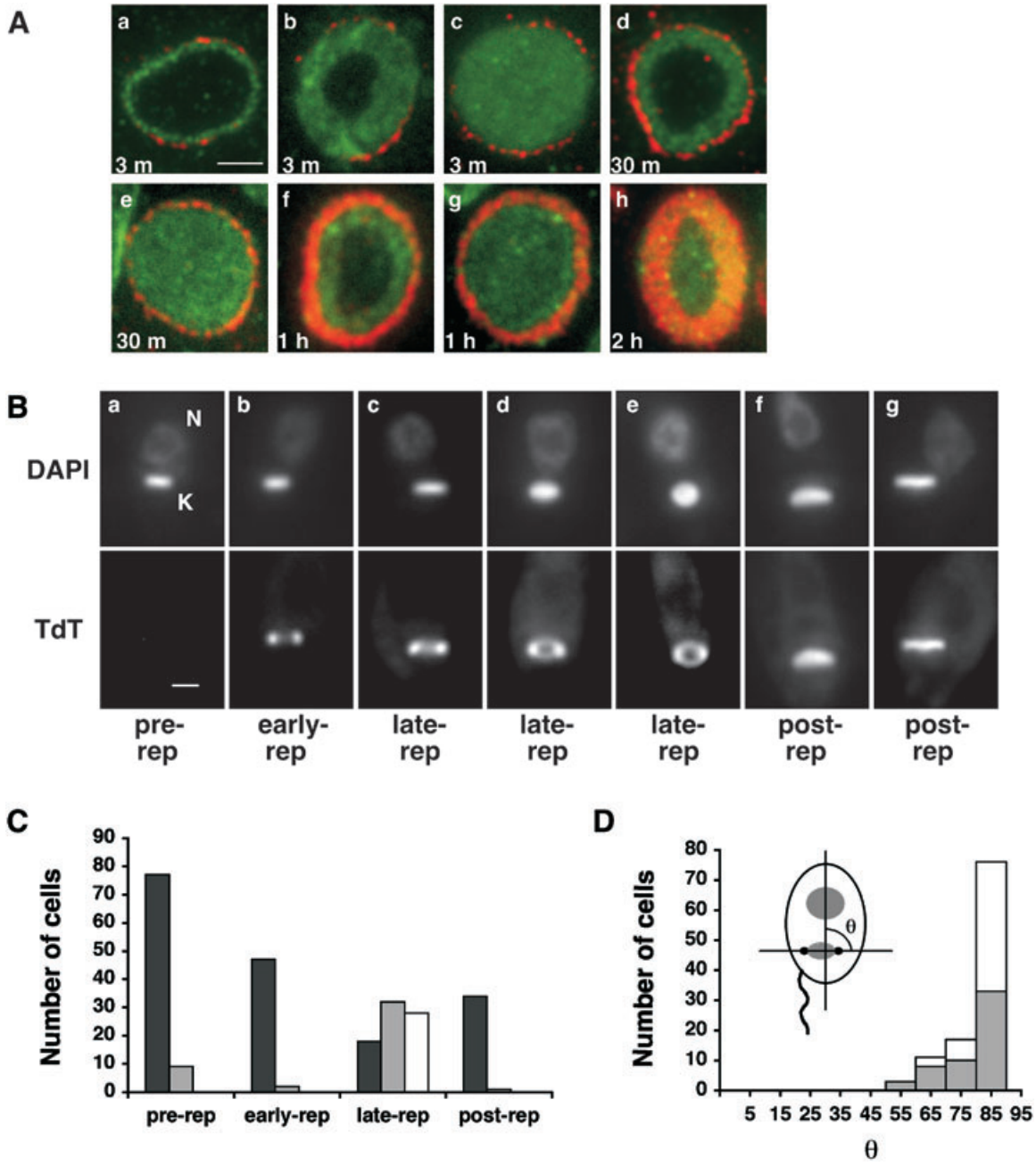

Fig. 1. Fluorescence analysis of *C. fasciculata* kDNA.
A. BrdU and TdT labelling of isolated *C. fasciculata* networks. Cells were metabolically labelled with BrdU (red) for the indicated time (m, min; h, hour), and after network isolation, the gapped minicircles (that had completed replication during the current cell cycle) were labelled with TdT (green). Bar, 3 μm.
B. *In situ* TdT labelling of kDNA in permeabilized *C. fasciculata* cells. Upper panel shows DAPI staining of both nuclear DNA (N) and kDNA (K). Lower panel shows TdT labelling of the same cells at different stages of kDNA replication as indicated. All TdT images are at same exposure. The strongly fluorescent spots flanking the kDNA disk are the two antipodal sites. The regions of weak fluorescence are the gapped minicircles on the network. We did not detect double-size networks (as in panels f and g) that are TdT negative, indicating that gap repair occurs simultaneously with network scission. Bar, 1 μm.
C. Reorientation of the kinetoplast during the *C. fasciculata* replication cycle. Black bars indicate kDNA disks perpendicular to focal plane and viewed from 'edge'; white bars indicate kDNA disks in the 'flat' configuration, parallel to the focal plane; grey bars show 'intermediate' configuration of kDNA disk. The relative per cent of each stage is not represented on the graph; of the cells with one kinetoplast, prereplication cells constitute 66% of the total, early replication cells, 9%, late-replication cells, 20%, and post-replication cells, 5%.
D. Positioning of the antipodal sites in *C. fasciculata* cells. Inset diagram defines θ, the angle between a line connecting the antipodal sites (determined from a TdT image) and a line traversing the centre of the cell (determined from a phase image). Grey bars illustrate the values of θ for antipodal sites in cells with 'edge' configuration; white bars illustrate the values of θ in cells with 'flat' and 'intermediate' configurations.

the kDNA disk; these must be in the early stages of network replication. The examples in panels c, d and e had TdT labelling of the antipodal sites and also considerable labelling of the kDNA disk; these must be in the later stages of replication. Finally, kinetoplasts like those in panels f and g had no label in the antipodal sites but there was label of the kDNA; these kinetoplasts, with a diameter greater than that in panel a, had completed replication of minicircles but had not yet undergone gap repair.

Analysis of images like those in Fig. 1B led to two important new conclusions. First, we found that the kDNA disk can have different orientations in the cell. In some cells the disk is perpendicular to the focal plane and therefore visualized on its edge (examples are in panels a, b, c and g); in other cells the disk's flat surface is oriented parallel to the focal plane (examples are in panels d and e). In the remaining cells the disk has an intermediate orientation (an example is in panel f). Remarkably, the disk is visualized predominantly from its edge in all stages except during late replication (see bar graph in Fig. 1C). Only at this stage, in which both the antipodal sites and the kDNA were labelled, was the disk in many cells oriented with its flat surface parallel to the focal plane. Thus, the kDNA disk reorients at a specific time in its replication cycle.

The second conclusion concerns the positioning of the antipodal sites. We measured the angle θ (defined in the inset of Fig. 1D) and found its mean value to be $82 \pm 9°$ (bar graph in Fig. 1D). Furthermore, the two antipodal sites were nearly always in the same focal plane (see examples in Fig. 1B) (Ferguson *et al*., 1992; Pérez-Morga and Englund, 1993b) implying that the cells have a preferred orientation on the microscope slide. Taken together, these data provide evidence that the antipodal sites are fixed in position, in three dimensions, during the entire replication cycle.

A surprising result with T. brucei *kDNA replication*

We next applied these methods to *T. brucei* (Fig. 2A). As expected, the green TdT fluorescence of isolated networks displays the polar distribution of gapped minicircles observed previously (Hoeijmakers and Weijers, 1980; Ferguson *et al*., 1994; Robinson and Gull, 1994; Guilbride and Englund, 1998). In these networks, the size of the fluorescent zones increases with extent of replication (compare green TdT label on networks a, b, c and d in Fig. 2A). Network a, which is approximately circular and has thin zones of green TdT label, is in an early stage of replication, networks b and c, which are elongated and have thicker zones of TdT label, are in later stages, and network d, which is dumbbell shaped and uniformly labelled with TdT, is in the last stage just prior to network division. The red BrdU labelling, marking the two sites on the network containing minicircles replicated during the 3 min pulse, were always positioned, as in *C. fasciculata*, ~180° apart, consistent with minicircle attachment next to the antipodal sites. Although the two red BrdU spots were always within the green TdT-labelled region, it was surprising that they were not always at the network poles (Fig. 2A). For example, with a 3 min BrdU labelling (Fig. 2A, networks a, b, c, and d), the red fluorescence is concentrated in two small spots whose axis is usually rotated relative to the network's major axis. This finding, confirmed in networks labelled with BrdU for longer times (Fig. 2A, networks e to p), raises the possibility that the network is not stationary during replication as previously thought, but that it might oscillate back and forth, allowing minicircles to attach sequentially along the periphery near the network poles (see model in Fig. 2B).

Because acid treatment required for visualizing BrdU epitopes usually reduces the quality of TdT labelling, we conducted another experiment in which the networks had been labelled only with BrdU and DAPI (Fig. 3); in this favourable preparation we could clearly characterize over 90% of the networks. For labelling times of 15, 30, 45, 60 and 90 min, we examined 70–200 networks, and at each time point between 15 and 21% were BrdU-labelled. To further characterize kinetoplast motion, we focused on networks in later stages of replication that are either elongated or ultimately dumbbell-shaped (see Fig. 3 for examples). In those cases it was straightforward to determine if BrdU incorporation was at the network poles or displaced from the poles. Of 53 elongated networks, 18 had BrdU incorporation at the poles (examples are networks a, g, n and r) whereas 35 had incorporation displaced from the poles (examples are networks b, c, f and x), consistent with an oscillating kinetoplast. Networks cc and dd, having only a single region of red BrdU fluorescence and being small in size, likely segregated from a double-size network during the labelling period; these forms constituted 20% of the networks labelled with BrdU for 2 h.

Further analysis of the BrdU-labelled networks in Figs 2A and 3 provide more information about kDNA replication. As expected, the amount of BrdU fluorescence increases with the time of labelling. The arc of peripheral red fluorescence increases in length, especially during the first 15 min, and it also begins to thicken. Only in networks in later stages of replication, labelled for longer times (networks i–p; Fig. 2A), does the BrdU-labelled zone cover half or more of the periphery of the green TdT-labelled region of the network. These facts indicate that oscillations do not extend over the entire periphery in the TdT labelled regions, but instead are restricted to a local region. After several oscillations in one region of the network periphery, causing thickening of the

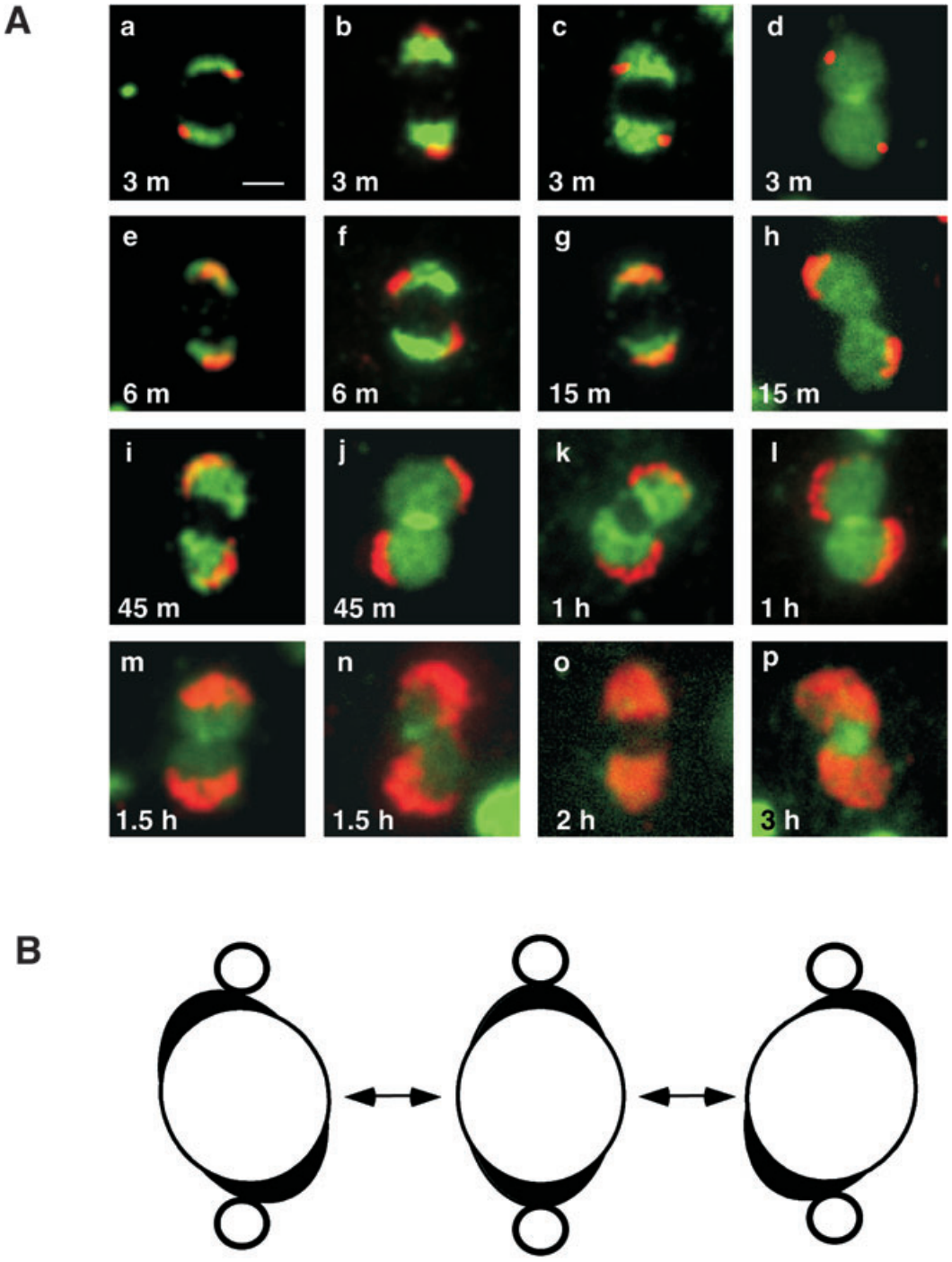

Fig. 2. Replication of *T. brucei* kDNA.
A. Fluorescence analysis of isolated *T. brucei* networks. Cells were metabolically labelled with BrdU (red) for the indicated time (m, min; h, hour). After isolation the networks were TdT labelled (green). In network o, the BrdU labelling and TdT labelling were coincident. Bar, 2 μm.
B. Diagram showing kinetoplast oscillations. The large ellipse is the kDNA disk with black regions containing newly replicated gapped minicircles. The small circles are antipodal sites containing the topoisomerase II that attaches gapped minicircle progeny to the network. In this diagram, the oscillations are centred around the networks' poles; after multiple oscillations (the number is not known), the network jumps to a new position causing minicircles to attach at another segment of the periphery.

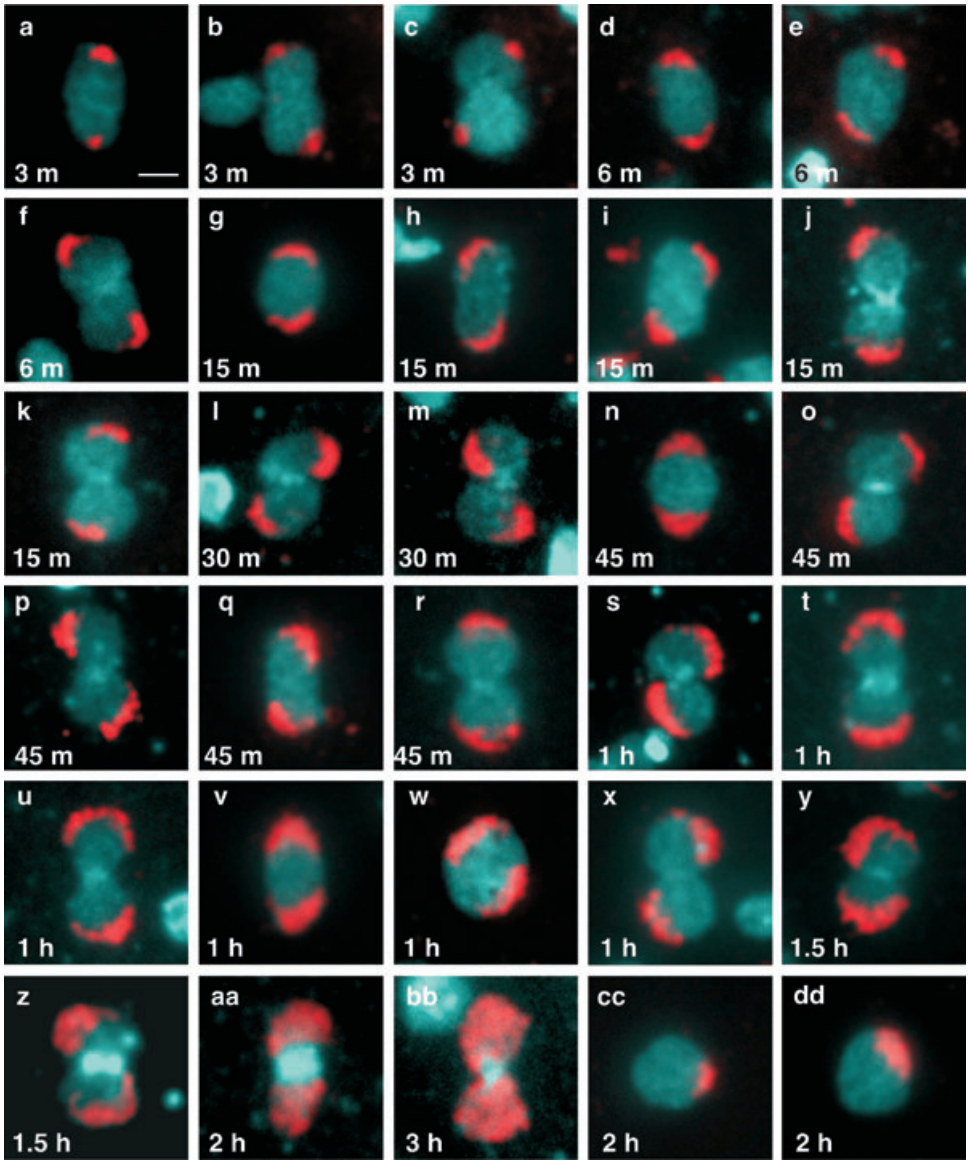

Fig. 3. BrdU immunofluorescence in isolated *T. brucei* networks. Images show BrdU labelling (red) and DAPI staining (blue). Labelling times are indicated. Only images of elongated or dumbbell-shaped networks are shown because it is possible to tell if BrdU labelling is at the poles (as in network a) or displaced from the poles (as in network b). The bright blue DAPI staining in the centre of some dumbbell-shaped networks (especially networks o, z, aa and bb) is probably due to maxicircles which concentrate in this position just prior to network division (Hoeijmakers and Weijers, 1980). Bar, 2 μm.

BrdU zone, the network apparently displaces to another region and then resumes oscillations. We refer to the network displacements as jumps. Therefore, minicircle reattachment involves alternating oscillations and jumps.

Pulse-chase and pulse-chase-pulse labelling of T. brucei *kDNA with BrdU*

To provide further insight into kDNA replication, we next conducted pulse-chase experiments. Figure 4A shows networks pulse-labelled with BrdU for times ranging from 3 to 60 min, and then chased for 2 h. After isolation the networks were TdT-labelled. Microscopy revealed in all examples an apparent inward migration of the BrdU-labelled minicircles (red) during the chase. This apparent migration is explained by continuous removal of unreplicated covalently closed minicircles from the network interior (between the two labelled zones) and attachment of their unlabelled progeny at the ends of the network. The asymmetric positioning of the BrdU labelling (in networks a, c, d and f) is due to kinetoplast oscillation and jumping. Network g has only a single region of red BrdU fluorescence; it is visualized by DAPI staining because it is TdT-negative. Like networks cc and dd in Fig. 3, it must

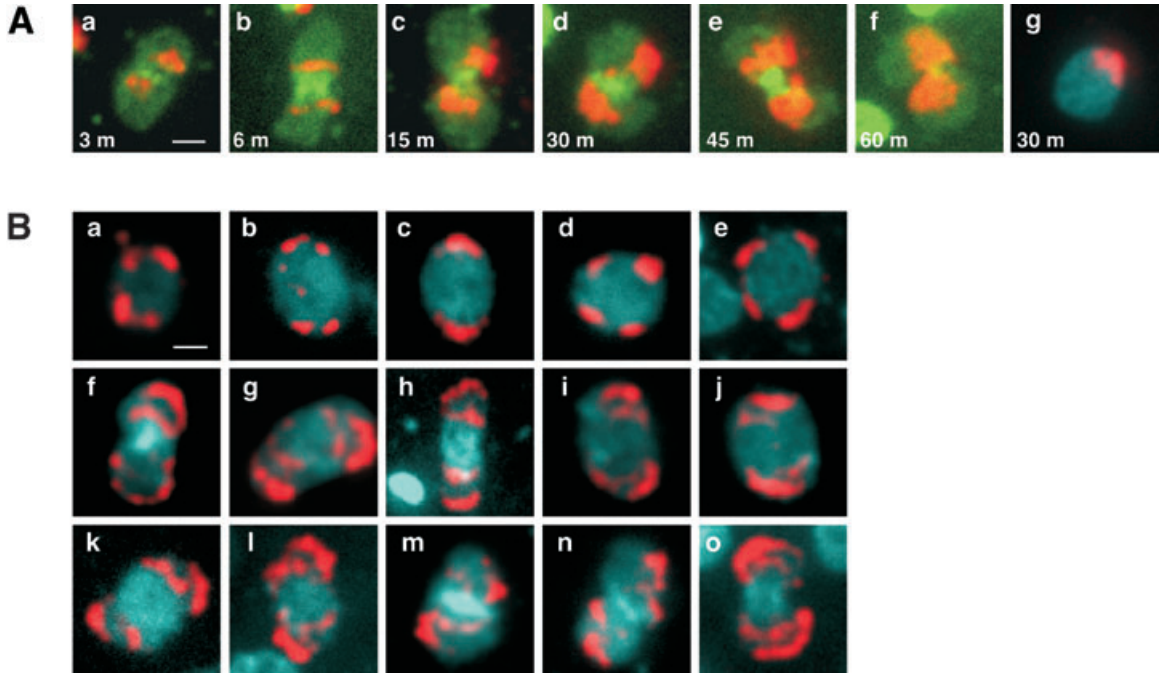

Fig. 4. Pulse-chase labelling of *T. brucei* networks with BrdU.
A. Pulse-chase labelling of *T. brucei* networks with BrdU. Cells were labelled with 50 μM BrdU (red) for the indicated time and then chased with 50 μM thymidine for 2 h. The isolated networks were TdT labelled (green) and visualized by fluorescence microscopy. Network g did not label with TdT and is stained with DAPI (blue). Bar, 2 μm.
B. Pulse-chase-pulse labelling with BrdU (red). Cells were pulse-labelled with 50 μM BrdU, then chased with 100 μM thymidine, and finally pulse-labelled again with 150 μM BrdU. The networks were also DAPI-stained (blue). The time-course was: (a–c), pulse-3 min, chase-10 min, pulse-3 min; (d–e), pulse-3 min, chase-30 min, pulse-3 min; (f–o), pulse-10 min, chase-60 min, pulse-20 min Bar, 2 μm.

have segregated during the chase from a double-size network and its minicircle gaps must then have been repaired, rendering it TdT negative.

Figure 4B shows networks labelled with BrdU in pulse-chase-pulse experiments. Networks a–c were pulsed for 3 min, chased for 10 min, and pulsed again for 3 min. Near each pole of networks a and b are two peripheral red BrdU spots. One must have been labelled during the first pulse, and then, during the chase, kinetoplast movement resulted in labelling during the second pulse at a nearby site. In network c, two peripheral spots at each pole cannot be resolved, possibly because kinetoplast movement reversed direction during the chase so that labelling during the second pulse would be very close to that of the first. Alternatively, the two spots may simply not have resolved, possibly because of incomplete wash-out of BrdU during the chase; this possibility may explain many cases as networks like that in panel c are five times more abundant than the type shown in panels a and b. Networks d and e were pulsed for 3 min, chased for 30 min and pulsed again for 3 min. The longer chase used for these examples caused the two labelled spots at each pole to be further apart than those in networks a and b. Networks f to o were pulsed 10 min with 50 μM BrdU, chased 60 min with 100 μM thymidine, and then pulsed again with 150 μM BrdU for 20 min. The increased BrdU concentration and longer labelling time strengthened the BrdU signal in the second pulse, an effect most striking in networks g, i, j, l, m and o. In all of these cases the stronger BrdU labelling is at the network periphery whereas the weaker label has moved inward as more minicircles had been attached to the periphery during the chase and the second pulse. In most of these networks (e.g. i, j, k, l, m, n and o) the inner labelling arc is displaced from the outer because the site of local oscillations had jumped from one position to another. All of these data provide strong evidence for a kinetoplast that oscillates locally and then, after jumping to a new position, resumes local oscillation.

In-cell TdT labelling of T. brucei

Figure 5A shows images of TdT- and DAPI-stained *T. brucei* cells at different stages of kDNA replication. As with *C. fasciculata* (Johnson and Englund, 1998), the bright spots, enriched in multiply gapped free minicircles, colocalize with topoisomerase II (Fig. S1), and therefore must represent antipodal sites. The weakly staining regions are parts of the network containing minicircles with few gaps. Panel a shows a TdT-negative prereplica-

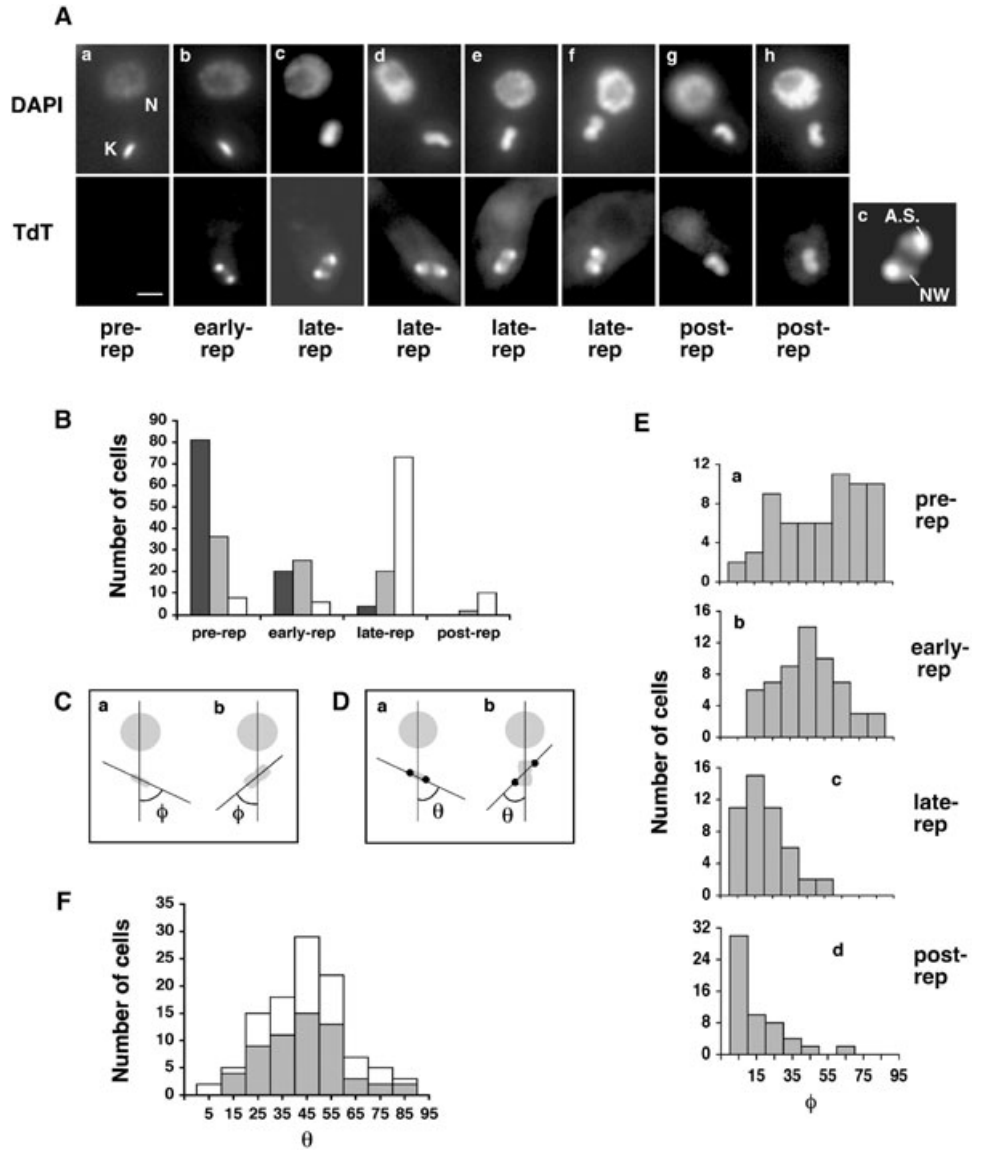

Fig. 5. In-cell fluorescence analysis of *T. brucei* kDNA replication.
A. *In situ* TdT labelling of *T. brucei* kDNA (Panel a–h). Upper panel shows DAPI staining of both nuclear DNA (N) and kDNA (K). Lower panel shows TdT-labelled kinetoplasts at different stages of replication. The strongly fluorescent spots flanking the kDNA disk are the two antipodal sites. The regions of weak fluorescence are the gapped minicircles on the network. Right hand panel shows enlargement of kinetoplast from panel c (A.S., antipodal sites; NW, network). Bar, 2 μm.
B. Reorientation of the kinetoplast during the replication cycle. Black bars indicate kDNA disks oriented perpendicular to the focal plane and viewed from 'edge'; white bars indicate kDNA disks oriented parallel to the focal plane and viewed from the 'flat' surface; grey bars indicate kDNA disks in 'intermediate' configuration. The relative per cent of each stage is not represented on the graph; of the cells with one kinetoplast, prereplication cells constitute 69% of the total, early replication cells, 8%, late-replication cells, 19%, and post-replication cells, 4%.
C. Diagram defining ϕ, the angle between the major axis of the kDNA disk and the line connecting the centre of the nuclear DNA and kDNA. a, kinetoplast DNA in pre and early replicating stage; b, kinetoplast DNA in late and post-replicating stage.
D. Diagram defining θ, the angle between a line connecting the antipodal sites and a line connecting the centre of the nuclear DNA and kDNA. a, kinetoplast DNA in early replicating stage; b, kinetoplast DNA in late replicating stage.
E. Positioning of the kDNA disk, as determined by the angle ϕ, at different stages of the *T. brucei* kDNA replication cycle.
F. Positioning of the antipodal sites in *T. brucei* cells. Grey bars illustrate values of θ for antipodal sites in early replicating stage cells; white bars illustrate values of θ in late replicating stage cells.

tion cell. Panel b shows a cell in the early stage of replication, which has TdT labelling in the antipodal sites but little in the network. Panels c, d, e and f show cells in the late stages of replication with labelling of both the antipodal sites and the kDNA. Note that the antipodal sites in panels c, e and f are positioned asymmetrically, as expected for an oscillating kinetoplast (see Fig. S2 for more examples of asymmetrical positioning). Panels g

and h show cells that have completed replication of their minicircles (as they have no antipodal sites) and are undergoing segregation.

As with *C. fasciculata,* there was a reorientation of the kinetoplast during the replication cycle (Fig. 5B). At most stages of replication the kDNA disk was oriented either perpendicular to the focal plane (e.g. viewed from the 'edge') or in an intermediate position. However, like *C. fasciculata,* most cells in the late stage of replication (as well as post replication) were reoriented so that the disk's flat surface was parallel to the focal plane.

Another indication of kinetoplast reorientation comes from measurement of the angle ϕ (defined in the diagram in Fig. 5C). Prior to replication, with TdT-negative kinetoplasts, values of ϕ varied over a wide range with most between 20° and 90° (Fig. 5E, panel a). In the early stage of replication (panel b), ϕ is about 47°$\pm$20°, a distribution similar to that of the antipodal sites (compare with Fig. 5F). The asymmetric positioning of the antipodal sites provides evidence for kinetoplast oscillations *in vivo*. Although oscillations would not be detectable on kinetoplasts oriented perpendicular to the focal plane (viewed from 'edge'), asymmetric positioning of the antipodal sites is easily visible in those with intermediate or flat orientation (Fig. 5A). The kinetoplast disk continues to reorient in the late stages of replication, with the value of ϕ decreasing to 20 $\pm$ 13° (Fig. 5E, panel c). In the post-replication kinetoplasts, still TdT-positive but without antipodal sites, ϕ decreases further to 14 $\pm$ 5° (Fig. 5E, panel d).

We also evaluated the position of the antipodal sites by measuring θ (defined diagrammatically in Fig. 5D). We found that θ has a mean value of 49 $\pm$ 16° for early stages of replication and 46 $\pm$ 18° for late stages (Fig. 5F). As with *C. fasciculata,* the two antipodal sites are almost always in the same focal plane (see examples in Fig. 5A and supplementary Fig. S2), implying that the cells have a preferred orientation on the slide. Since values of θ are similar at all stages of replication, we conclude, as with *C. fasciculata,* that the antipodal sites are fixed within the cell.

The effect of SSE1 RNAi on the T. brucei *replication mechanism*

We next applied the BrdU/TdT-labelling method to networks from cells in which expression of structure-specific endonuclease I (SSE1) (Engel and Ray, 1998; Liu *et al*., 2005b) had been silenced by RNAi. SSE1 is localized in the antipodal sites and is involved in removal of replication primers. RNAi of SSE1 causes shrinking of the network and persistence of the gaps in network minicircles (Liu *et al*., 2005b). Unexpectedly, we found using TdT labelling that the structure of isolated replicating networks differed markedly from those from wild-type cells (Fig. 6A). Instead of polar labelling (as shown for wild type cells by the green TdT fluorescence in Fig. 2A), the TdT labelling after 2 days of RNAi was distributed in peripheral rings (Fig. 6A, upper panel) resembling those in replicating *C. fasciculata* networks (Fig. 1A). As with *C. fasciculata* kDNA, the rings ranged from thin to thick. After 4 days of RNAi the isolated networks were smaller in size, but still formed rings (Fig. 6A, lower panel). At day 4 most rings were thin, like networks i–n; thicker rings like o, and uniformly labelled networks like p were rare, probably because network replication had slowed or stopped. To measure the frequency of ring formation, we evaluated ~1000 isolated networks (TdT-labelled and DAPI-stained) at different times of RNAi. Among TdT positive networks from cells not undergoing RNAi, 25% had polar TdT labelling and only 1% appeared to have a ring pattern (the rest were fully labelled unit size and double size networks). After 2 days of RNAi, only 4% of TdT-positive networks had polar labelling and 25% were rings. At day 4, none of the TdT-labelled networks had polar labelling and 67% were rings.

To study the mechanism of ring formation in RNAi cells we first evaluated whether the antipodal sites are still functional in networks with the ring configuration. For this purpose, we combined BrdU labelling with TdT labelling of isolated networks (Fig. 6B, networks a–l). Short pulse labellings with BrdU resulted in red fluorescence positioned in two peripheral regions ~180° apart when the green TdT fluorescence formed a peripheral ring. This BrdU labelling pattern provides strong evidence that in ring-forming cells, the newly replicated minicircles attach to the network exclusively at positions adjacent to the antipodal sites. As the labelling time increases, the zones of red BrdU fluorescence expand along the periphery until they ultimately merge, forming a ring. The rings thicken in networks labelled with BrdU for longer periods (Fig. 6B, networks m–u; these networks were not TdT-labelled).

Inspection of the rings, labelled with either BrdU or TdT, revealed some important characteristics. Some networks have split rings, with small openings containing little or no detectable label separating the two TdT- or BrdU-labelled zones (examples are network k in Fig. 6A and networks m and n in Fig. 6B). Other networks, at a more advanced stage of replication, have the ring openings filled in, but instead have alternating thick and thin zones (examples are networks b, d, e, f and j in Fig. 6A and networks q, r and s in Fig. 6B).

To investigate the structure of kDNA *in situ*, we conducted TdT labelling of intact cells that had undergone RNAi for 2 days. Figure 6C shows examples of cells at different stages of kDNA replication that had been DAPI-stained (upper panel) and TdT-labelled (lower panel). In each example of a cell in the late replication stage the TdT label forms a ring structure and each ring is associated

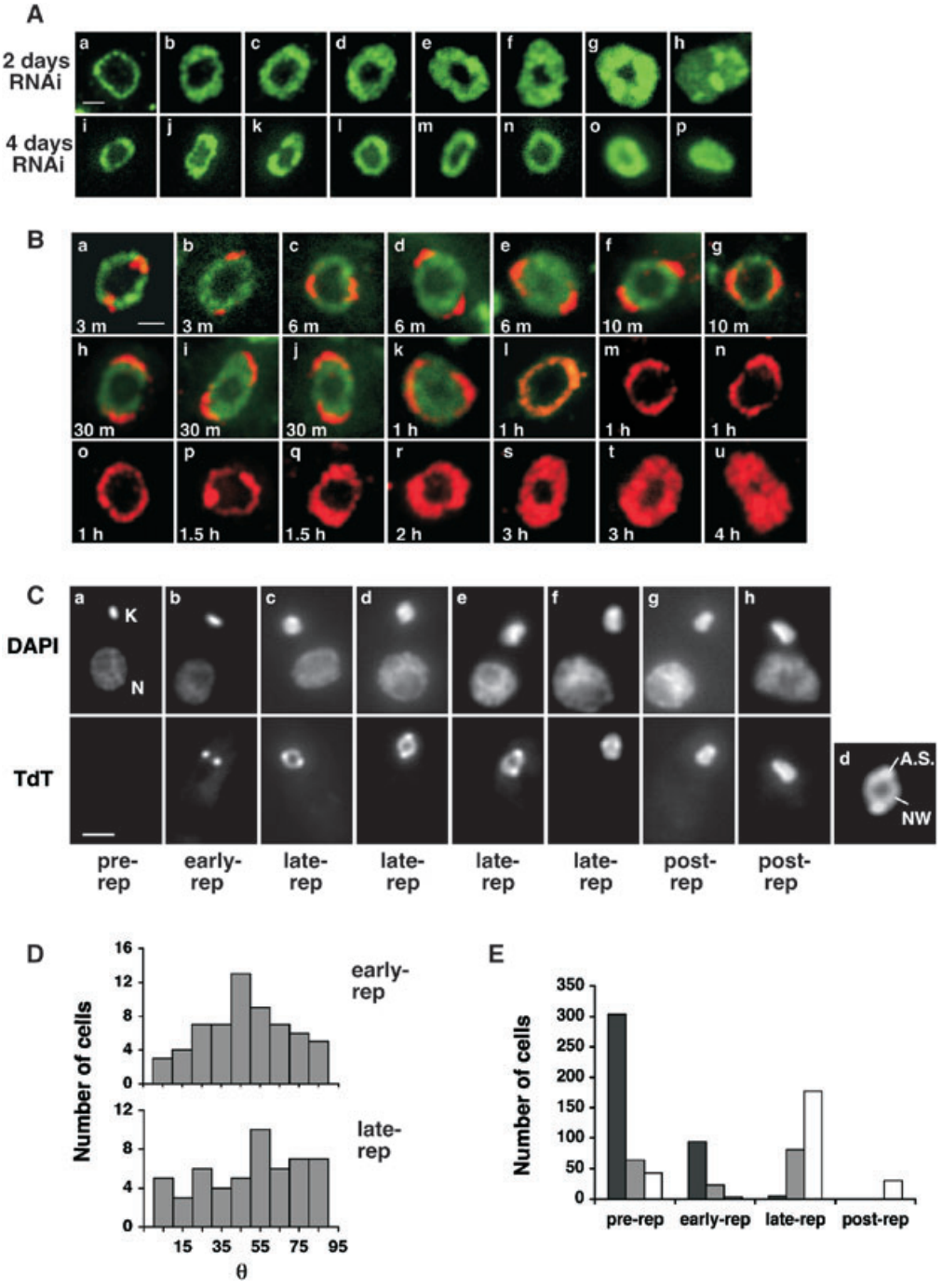

Fig. 6. kDNA networks in *T. brucei* after knockdown of SSE1 by RNAi.
A. TdT labelling (green) of isolated networks from RNAi cells (induced for 2 and 4 days). Bar, 2 μm.
B. BrdU labelling (red) combined with (panels a–l) or without (panels m–u) TdT labelling (green) in isolated networks after 2 days of RNAi. Labelling times are indicated. In network l, the BrdU labelling and TdT labelling are coincident. Bar, 2 μm.
C. *In situ* TdT labelling in cells after 2 days of RNAi silencing of SSE1. Upper panel shows DAPI staining of both nuclear DNA (N) and kDNA (K) in cells undergoing RNAi of SSE1 for 2 days. Lower panel shows TdT labelling. Bright fluorescent spots are antipodal sites and more weakly fluorescent rings are gapped minicircles on network. Right hand panel is enlargement of network in Panel d. Bar, 2 μm.
D. Position of antipodal sites in cells undergone RNAi for 2 days. θ is defined as in Fig. 5D. Upper graph shows values of θ for cells in early stages of replication, and lower graph shows values for cells in the late stages.
E. Reorientation of the kinetoplast during the replication cycle in cells after 2 days of RNAi silencing of SSE1. Black bars show 'edge' configuration of kDNA disk; white bars show 'flat' configuration of kDNA disk; grey bars show 'intermediate' configuration of kDNA disk. The relative per cent of each stage is not represented on the graph; of the cells with one kinetoplast, prereplication cells constitute 48% of the total, early replication cells, 14%, late-replication cells, 31%, and post-replication cells, 7%.

with two bright spots corresponding to the antipodal sites. These results are consistent with the BrdU/TdT labelling pattern in isolated networks (Fig. 6B) and provides more evidence that the antipodal sites are functional in the RNAi cells.

We next measured the position of the antipodal sites in cells that had undergone RNAi for 2 days (Fig. 6D). We measured the angle θ (defined in Fig. 5D) in 114 cells. Whereas the value of θ in wild type cells centred on ~50° in both early and late stages of replication (Fig. 5F), in the RNAi cells the distribution of θ was more disperse, especially during the later stages of replication. We also found, as in wild type (Fig. 5B), that the kDNA disk reoriented during the replication cycle, with most of those in the late stage of replication, as well as post replication being in the 'flat' configuration (Fig. 6E).

Discussion

The T. brucei *kinetoplast oscillates and jumps*

We have re-investigated *T. brucei* kDNA replication using fluorescence microscopy of isolated networks (Figs 2A and 3). Our results indicate that the replicating network is not stationary, but that it oscillates back and forth (see model in Fig. 2B). Support for an oscillating kinetoplast also comes from TdT labelling of permeabilized intact cells (Fig. 5A). Further analysis of fluorescent images in Fig. 2A indicates that oscillations must be limited in amplitude as the BrdU labellings usually encompass half or less of TdT-labelled zones. The length of the BrdU arc along the network periphery increases with time of labelling, especially during the first ~15 min; then peripheral elongation slows down and the BrdU zone thickens (Figs 2A and 3). Even after labelling with BrdU for 1.5 h (networks m and n in Fig. 2A), the BrdU labelling encompasses only part of the network periphery that is TdT labelled. These facts imply that in addition to oscillations, minicircle attachment also involves displacement of the kinetoplast to a new position, a process we call jumping. After a jump, the kinetoplast can resume local oscillation at a new position on the network periphery. We do not yet know the amplitude of the oscillations, the number of oscillations that occur before a jump, the length of a jump, or the number of jumps that occur in each replication cycle. However, our studies on SSE1 RNAi cells (Fig. 6) indicated that these parameters may vary under different conditions (discussed later).

Further evidence for kinetoplast motion comes from pulse-chase-pulse experiments (Fig. 4B). When a chase separates two 3 min BrdU labellings, there often are two BrdU sites near each pole of the network, consistent with movement of the kDNA disk during the chase. The spacing of the two spots generally increases with chase time. With a chase of 60 min, BrdU label from the first pulse moves inward because unlabelled minicircles were attached to the periphery during the chase. During the second pulse, BrdU-labelled minicircles are again attached to the periphery, resulting in layers of BrdU label near each pole of the network. In most examples the BrdU-labelled minicircles attached during the second pulse were displaced laterally from those incorporated during the first; this displacement is likely due to jumping.

The antipodal sites do not move

The *C. fasciculata* antipodal sites appear fixed in three dimensions throughout the entire replication cycle. This conclusion is based on the fact that they are invariably in the same focal plane (Fig. 1B) and that the angle θ (defined in Fig. 1D) is in a narrow distribution around 82° (Fig. 1D). The same conclusion very likely applies to *T. brucei* although θ (defined in Fig. 5D) varies over a wider range of values (Fig. 5F). Because the *T. brucei* kinetoplast is considerably smaller than that from *C. fasciculata*, part of this variation could be due to inaccuracies in measuring θ. Taken together, these facts provide strong support for the idea that the kinetoplast rotates or oscillates between fixed antipodal sites and seem to rule out the possibility that the antipodal sites move along the perimeter of a stationary kDNA disk.

A crucial question is whether the *C. fasciculata* kDNA disk actually rotates as we had previously concluded, or whether it also undergoes oscillations/jumps of 180° like the *T. brucei* RNAi cells described in Fig. 6. In our previous report on *C. fasciculata* kinetoplast rotation, we argued against oscillation because none of the EM-autoradiographs suggested a change in direction of motion during a pulse labelling (Pérez-Morga and Englund, 1993b). Also, as mentioned above, TdT labelling of *C. fasciculata* networks always reveals a ring of uniform thickness unlike the split rings common in *T. brucei* RNAi cells. Based on the results in this article we tentatively conclude that kDNA replication in *T. brucei* and *C. fasciculata* both involve kinetoplast movement, but the motion, either oscillation or rotation, differs in the two parasites.

It is remarkable that a structure as large as a kinetoplast disk could oscillate or rotate, and therefore we wondered whether our data could be explained by a model that did not involve movement of either the kDNA disk or antipodal sites. For example, minicircles could initially be attached to a non-moving network adjacent to fixed antipodal sites, and then they could be directionally transported, most likely by successive decatenations and recatenations, to other sites in the network. In our previous report on kinetoplast rotation in *C. fasciculata,* we considered a similar alternative model and presented strong arguments

against it (Pérez-Morga and Englund, 1993b). In *T. brucei,* the alternative model could explain the peripheral labelling detected after a short BrdU pulse, but it is difficult to imagine how it could account for the longer-time or pulse-chase labellings that we observed. The major problem is that jumps are required to explain the latter patterns of BrdU labelling, and by the alternative model it is difficult to understand how minicircles could be transported to a distant site. It is even more difficult to explain the observed symmetry of BrdU labellings; the alternative model would require similar patterns of minicircle transport to be co-ordinated at each end of the network. Both of these problems are easily resolved if the jumps involve a partial rotation of the kDNA disk. Based on these considerations, we believe that the most likely explanation of our data is that the *T. brucei* kinetoplast disk actually oscillates and jumps during its replication.

We also discovered another form of kDNA motion involving reorientation of the kDNA disk. Although kDNA disks in both *C. fasciculata* and *T. brucei* are usually positioned perpendicular to the focal plane (in the 'edge' configuration), we had noted in the past some with the disk parallel to the focal plane (in the 'flat' configuration) (Johnson and Englund, 1998). Now we have found in both parasites that disk reorientation occurs in most cells at a specific time in the cell cycle, mainly during the later stages of kDNA replication (Figs 1C and 5B). We also detected reorientation of the kDNA disk by measurement of the angle ϕ (defined in Fig. 5C). ϕ changed significantly during the *T. brucei* kDNA replication cycle (Fig. 5E).

RNAi of replication proteins alters kinetoplast motion

While investigating the effect of RNAi on SSE1 (Liu *et al*., 2005b), we made the unexpected discovery that recently replicated minicircles (as visualized by TdT labelling) are localized not at the network poles, as in wild-type networks, but in peripheral rings that superficially resemble those in *C. fasciculata* networks (Fig. 6A). After 2 or 4 days of RNAi nearly all of the TdT-labelled networks were rings even though those from day 4 had shrunk in size. The small size is due to the fact that minicircles had been released from the network for replication but reattachment of gapped progeny was delayed because primer removal was incomplete (Liu *et al*., 2005b).

We considered three possibilities to explain the appearance of rings. One is that the antipodal sites had degenerated, allowing gapped minicircles to be attached around the entire network periphery. A second is that kinetoplast motion had actually switched from oscillation to rotation. A third is that the amplitude of oscillation/jumping had increased to 180°, giving the appearance of a ring without fundamentally changing the mechanism. We used TdT and BrdU labelling (Figs. 6A and B) to distinguish between these possibilities. The finding that a 3 min pulse with BrdU labelled two peripheral sites ~180° apart indicated that the antipodal sites are functional in the RNAi cells and ruled out the possibility that gapped minicircles are attached around the entire network periphery. The visualization of antipodal sites by in-cell TdT labelling (Fig. 6C) confirms this conclusion.

We next addressed the other two possibilities, that RNAi caused the kinetoplast to rotate or that it caused an increase in amplitude of oscillation/jumping. Longer labellings with BrdU (1 h or more) produced very few rings of uniform thickness (one example is network t in Fig. 6B). Most networks either had split rings (Fig. 6B, networks m and n) or rings that have alternating thick and thin regions (Fig. 6B, networks q, r, s and u). In *C. fasciculata,* all the networks have rings of uniform thickness (see examples in Fig. 1A), which are compatible with a rotating kinetoplast. The predominance of split rings or rings of variable thickness indicates either that network oscillations had increased in amplitude or that the amplitude of the oscillations may have remained relatively small but the frequency or magnitude of jumps could have increased. Either possibility could explain how minicircles are attached almost completely around the network periphery. Either mechanism also explains why the replicating networks in RNAi cells are approximately circular in shape rather than having the elongated or dumbbell structure found in wild-type cells.

It is not clear how RNAi of SSE1 causes this change in attachment of minicircles around the network. It is unlikely related to SSE1′s enzymatic activity, as we also found rings after RNAi of p38, another replication protein localized to the antipodal sites (Liu *et al*., 2006; Y. Liu and P.T. Englund, unpubl. data). The same is true following RNAi of DNA polymerase β-PAK, an enzyme localized within the kDNA disk (Saxowsky *et al*., 2003; Z. Zhao and P.T. Englund, unpubl. data). However, RNAi of the antipodal topoisomerase II (Melendy *et al*., 1988), and DNA ligase kα, that localize within the kDNA disk (Downey *et al*., 2005), does not cause ring production (Y. Liu and P.T. Englund, unpubl. data). Because most kDNA replication proteins are organized in discrete sites around the kDNA disk and presumably interact with each other, it is possible that RNAi-induced depletion of some of these proteins causes changes in these interactions, thereby affecting proteins involved in kinetoplast motion.

Conclusion

As discussed in the Introduction, a key feature of kDNA replication must be a mechanism ensuring that the progeny of a replicating free minicircle segregate with high probability to each of the two daughter networks. Accurate segregation would prevent loss of essential

minicircles, and we have speculated previously that kinetoplast rotation could contribute to this process (Klingbeil *et al*., 2002b). However, with the elongated or dumbbell-shaped network in *T. brucei,* it is not clear how oscillation could help segregate sister minicircles except to make the replication process more orderly, allowing the newly replicated minicircles to attach along the network periphery rather than piling up at one point. Kinetoplast motion also determines the ultimate shape of the replicating network, approximately circular in *C. fasciculata* and elongated and ultimately dumbbell-shaped in *T. brucei.* As for the mechanism of minicircle segregation, our current speculation is that sister minicircles segregate in the KFZ and these progeny migrate to different antipodal sites where they attach to opposite sides of the replicating network.

There is much to be learned about the mechanism of kinetoplast motion, and it is very likely that the attachment of the kDNA to the flagellar basal body via a *trans*-membrane filament system (Robinson and Gull, 1991; Ogbadoyi *et al*., 2003) impacts on the mechanism. Further progress in understanding kinetoplast motion is most likely to involve *T. brucei* because it is the only kinetoplastid parasite for which both reverse and forward genetic methods are available.

Experimental procedures

Cells and RNAi

Crithidia fasciculata was grown at room temperature in brain heart infusion medium containing 20 μg ml^{-1} haemin, penicillin (Sigma, 100 units ml^{-1}) and streptomycin (Sigma, 0.1 mg ml^{-1}). Procyclic *T. brucei* (strain 29-13, a gift from Dr George Cross, Rockefeller University) was grown at 27°C in SDM-79 medium (Brun *et al*., 1979) supplemented with 10% fetal bovine serum. For RNAi of SSE1, this cell line was transfected with a stem-loop vector (Liu *et al*., 2005b).

Fluorescence labelling of kDNA

For metabolic labelling of *C. fasciculata*, BrdU and 2′-deoxycytidine (both 50 μM) were added to 1.0 ml of mid-log phase culture (3 to 5×10^7 cells ml^{-1}) with vigorous shaking. The 2′-deoxycytidine was included as dBrUTP can potentially reduce the production of dCTP in reactions involving ribonucleotide reductase (Kornberg and Baker, 1992). The labelled cells were chilled, harvested by brief centrifugation in a microcentrifuge at 4°C, and frozen in dry ice-ethanol. Similar conditions were used for labelling *T. brucei* (5 ml culture; 3 to 5×10^6 cells ml^{-1}; 27°C). For pulse-chase labelling of *T. brucei*, the cells were first incubated with 50 μM BrdU/2′-deoxycytidine as described above. Then they were microcentrifuged (1 min; room temperature) and resuspended in the same volume of medium containing 50 μM thymidine. For pulse-chase-pulse experiments, the cells were incubated with BrdU/2′-deoxycytidine, then with thymidine, and finally again with BrdU/2′-deoxycytidine. See Fig. 4 legend for details.

Our standard procedure is to pulse-label *in vivo* with BrdU, isolate (Pérez-Morga and Englund, 1993b) and TdT label the networks (Liu *et al*., 2005b), acid-treat to expose BrdU epitopes (1.5 M HCl, 20 min, room temperature), and detect these epitopes by immunofluorscence (Robinson and Gull, 1994). In the latter step, the networks were treated with Alexa Fluor 594-conjugated monoclonal anti-BrdU (Invitrogen), then with Alexa Fluor 594 goat anti-mouse IgG_1 (Invitrogen), and finally with DAPI (10 μg ml^{-1}). The treatment with 1.5 M HCl has detrimental effects on the kDNA network structure, making it somewhat difficult to find images like those in Fig. 2A. The effect is most severe on the TdT signal, and it varies among preparations. Damage is more severe for *T. brucei* networks than for those from *C. fasciculata*.

In-cell TdT labelling

In situ fluorescence labelling of gaps in network minicircles with TdT and Alexa Fluor 488-dUTP was performed as described (Liu *et al*., 2005b). Briefly, mid-log phase *C. fasciculata* or *T. brucei* cells were centrifuged at low speed, washed, and resuspended in PBS. Aliquots (5×10^5 cells in 25 μl of PBS) were spotted on poly-L-lysine-coated slides and allowed to adhere for 10 min at room temperature. Then cells were fixed in 4% paraformaldehyde in PBS for 5 min and washed twice in PBS containing 0.1 M glycine for 5 min at room temperature. After permeabilization in methanol overnight at –20°C, the cells were rehydrated with three 5 min washes in PBS. Then the cells were incubated (60 min, room temperature) in 25 μl TdT reaction buffer with 10 units of TdT, washed in 2 × SSC, and stained with DAPI (2 μg ml^{-1}). Slides were examined on an Axioskop microscope (Carl Zeiss). Images were captured with a charge-coupled device camera (RetigaTM Exi, QImaging) using IPLab software (Scanalytics).

Acknowledgements

We thank Dr Zefeng Wang for conducting preliminary studies that led to this project. We appreciate valuable advice from Drs Barbara Sollner-Webb, Terry Shapiro, Roger McMacken and members of our lab. We thank Gokben Yildirir for technical help. This research was supported by NIH Grant AI058613.

References

Abu-Elneel, K., Robinson, D.R., Drew, M.E., Englund, P.T., and Shlomai, J. (2001) Intramitochondrial localization of universal minicircle sequence-binding protein, a trypanosomatid protein that binds kinetoplast minicircle replication origins. *J Cell Biol* **153:** 725–734.

Brun, R., Jenni, L., Tanner, M., Schonenberger, M., and Schell, K.F. (1979) Cultivation of vertebrate infective forms derived from metacyclic forms of pleomorphic *Trypanosoma brucei* stocks. Short communication. *Acta Trop* **36:** 387–390.

Downey, N., Hines, J.C., Sinha, K.M., and Ray, D.S. (2005) Mitochondrial DNA ligases of *Trypanosoma brucei*. *Eukaryot Cell* **4:** 765–774.

Drew, M.E., and Englund, P.T. (2001) Intramitochondrial location and dynamics of *Crithidia fasciculata* kinetoplast minicircle replication intermediates. *J Cell Biol* **153:** 735–744.

Engel, M.L., and Ray, D.S. (1998) A structure-specific DNA endonuclease is enriched in kinetoplasts purified from *Crithidia fasciculata*. *Nucleic Acids Res* **26:** 4733–4738.

Engel, M.L., and Ray, D.S. (1999) The kinetoplast structure-specific endonuclease I is related to the 5′ exo/endonuclease domain of bacterial DNA polymerase I and colocalizes with the kinetoplast topoisomerase II and DNA polymerase beta during replication. *Proc Natl Acad Sci USA* **96:** 8455–8460.

Englund, P.T. (1978) The replication of kinetoplast DNA networks in *Crithidia fasciculata*. *Cell* **14:** 157–168.

Ferguson, M., Torri, A.F., Ward, D.C., and Englund, P.T. (1992) *In situ* hybridization to the *Crithidia fasciculata* kinetoplast reveals two antipodal sites involved in kinetoplast DNA replication. *Cell* **70:** 621–629.

Ferguson, M.F., Torri, A.F., Pérez-Morga, D., Ward, D.C., and Englund, P.T. (1994) Kinetoplast DNA replication: mechanistic differences between *Trypanosoma brucei* and *Crithidia fasciculata*. *J Cell Biol* **126:** 631–639.

Guilbride, D.L., and Englund, P.T. (1998) The replication mechanism of kinetoplast DNA networks in several trypanosomatid species. *J Cell Sci* **111:** 675–679.

Hoeijmakers, J.H.J., and Weijers, P.J. (1980) The segregation of kinetoplast DNA networks in *Trypanosoma brucei*. *Plasmid* **4:** 97–116.

Johnson, C.E., and Englund, P.T. (1998) Changes in organization of *Crithidia fasciculata* kinetoplast DNA replication proteins during the cell cycle. *J Cell Biol* **143:** 911–919.

Klingbeil, M.M., Motyka, S.A., and Englund, P.T. (2002a) Multiple mitochondrial DNA polymerases in *Trypanosoma brucei*. *Mol Cell* **10:** 175–186.

Klingbeil, M.M., Drew, M.E., Liu, Y., Morris, J.C., Motyka, S.A., Saxowsky, T.T., *et al.* (2002b) Unlocking the secrets of trypanosome kinetoplast DNA network replication. *Protist* **152:** 255–262.

Kornberg, A., and Baker, T.A. (1992) *DNA Replication.* New York, NY: W.H. Freeman.

Li, C., and Englund, P.T. (1997) A mitochondrial DNA primase from the trypanosomatid *Crithidia fasciculata*. *J Biol Chem* **272:** 20787–20792.

Liu, B., Liu, Y., Motyka, S.A., Agbo, E.E., and Englund, P.T. (2005a) Fellowship of the rings: the replication of kinetoplast DNA. *Trends Parasitol* **21:** 363–369.

Liu, B., Molina, H., Kalume, D., Pandey, A., Griffith, J.D., and Englund, P.T. (2006) Role of p38 in Replication of *Trypanosoma brucei* Kinetoplast DNA. *Mol Cell Biol* **26:** 5382–5393.

Liu, Y., Motyka, S.A., and Englund, P.T. (2005b) Effects of RNA interference of *Trypanosoma brucei* structure-specific endonuclease-I on kinetoplast DNA replication. *J Biol Chem* **280:** 35513–35520.

Melendy, T., Sheline, C., and Ray, D.S. (1988) Localization of a type II DNA topoisomerase to two sites at the periphery of the kinetoplast DNA of *Crithidia fasciculata*. *Cell* **55:** 1083–1088.

Ogbadoyi, E.O., Robinson, D.R., and Gull, K. (2003) A high-order trans-membrane structural linkage is responsible for mitochondrial genome positioning and segregation by flagellar basal bodies in trypanosomes. *Mol Biol Cell* **14:** 1769–1779.

Pérez-Morga, D., and Englund, P.T. (1993a) The structure of replicating kinetoplast DNA networks. *J Cell Biol* **123:** 1069–1079.

Pérez-Morga, D., and Englund, P.T. (1993b) The attachment of minicircles to kinetoplast DNA networks during replication. *Cell* **74:** 703–711.

Robinson, D.R., and Gull, K. (1991) Basal body movements as a mechanism for mitochondrial genome segregation in the trypanosome cell cycle. *Nature* **352:** 731–733.

Robinson, D.R., and Gull, K. (1994) The configuration of DNA replication sites within the *Trypanosoma brucei* kinetoplast. *J Cell Biol* **126:** 641–648.

Saxowsky, T.T., Choudhary, G., Klingbeil, M.M., and Englund, P.T. (2003) *Trypanosoma brucei* has two distinct mitochondrial DNA polymerase beta enzymes. *J Biol Chem* **278:** 49095–49101.

Shlomai, J. (2004) The structure and replication of kinetoplast DNA. *Curr Mol Med* **4:** 623–647.

Simpson, A.M., and Simpson, L. (1976) Pulse-labeling of kinetoplast DNA: localization of 2 sites of synthesis within the networks and kinetics of labeling of closed minicircles. *J Protozool* **23:** 583–587.

Simpson, L., Simpson, A.M., and Wesley, R.D. (1974) Replication of the kinetoplast DNA of *Leishmania tarentolae* and *Crithidia fasciculata*. *Biochim Biophys Acta* **349:** 161–172.

Stuart, K.D., Schnaufer, A., Ernst, N.L., and Panigrahi, A.K. (2005) Complex management: RNA editing in trypanosomes. *Trends Biochem Sci* **30:** 97–105.

Torri, A.F., and Englund, P.T. (1995) A DNA polymerase beta in the mitochondrion of the trypanosomatid *Crithidia fasciculata*. *J Biol Chem* **270:** 3495–3497.

Wang, Z., and Englund, P.T. (2001) RNA interference of a trypanosome topoisomerase II causes progressive loss of mitochondrial DNA. *EMBO J* **20:** 4674–4683.

Woodward, R., and Gull, K. (1990) Timing of nuclear and kinetoplast DNA replication and early morphological events in the cell cycle of *Trypanosoma brucei*. *J Cell Sci* **95:** 49–57.

Supplementary material

The following supplementary material is available for this article online:

Methods. Immunofluorescence of topoisomerase II and *in situ* TdT labeling.

For immunofluorescence, we used a guinea pig anti-topoisomerase II polyclonal antibody prepared against recombinant *T. brucei* topoisomerase II (a gift from Tom Kulikowicz and Terry Shapiro, Johns Hopkins University). Both wild type *T. brucei* 29-13 cells and cells which had undergone SSE1 RNAi for 2 days were centrifuged, washed once, and resuspended in PBS. Cells ($\sim 5 \times 10^5$ in 25 μl PBS) were spotted on a poly-lysine-coated slide and allowed to adhere for 10 min. Then cells were fixed and permeabilized in 75% ethanol for 2 h at 4°C, and then rehydrated with three 5 min washes in PBS. The slides were incubated with primary antibody against *T. brucei* topoisomerase II (diluted 1:50 in PBS containing 1% bovine serum albumin (BSA)) for 1 h at

room temperature. Following three 5 min washes in PBS, the slides were incubated with Alexa Fluor 594 goat anti-guinea pig secondary antibody (Invitrogen, 1:100 diluted in PBS with 1% BSA) for 1 h at room temperature. After three 5 min washes in PBS, the slide was subjected to terminal deoxynucleotidyl transferase (TdT) labeling as described in Experimental Procedures. The slides were stained with DAPI (2 μg/ml) and observed by fluorescence microscopy.

Fig. S1. Co-localization of the bright TdT-labeled spots with topoisomerase II.

Upper images show immunofluorescence localization of topoisomerase II. Lower images show TdT labeling of the same cells. These cells are ethanol fixed (see supplementary Experimental Procedures), a treatment that causes some shrinking of the kinetoplast. Use of 4% paraformaldehyde as a fixative did not shrink the kDNA but did cause spreading of the topoisomerase II spots. In some cells (not shown), the antibody detected topoisomerase II not only in the antipodal sites, but also in other sites near the kDNA disk; this observation is under further study. Bar, 1 μm.

Fig. S2. Fluorescence analysis of *T. brucei* kDNA replication. In-cell TdT labeling of *T. brucei* shows more examples of asymmetrical positioning of the antipodal sites in late replication stage cells. Right hand panel shows enlargement of kinetoplast from panel a (A.S., antipodal sites; NW, network). Bar, 2 μm.

This material is available as part of the online article from http://www.blackwell-synergy.com

Please note: Blackwell Publishing is not responsible for the content or functionality of any supplementary materials supplied by the authors. Any queries (other than missing material) should be directed to the corresponding author for the article.